SUPPORTING INFORMATION

On the structures of the rare-earth metal germanides from the series $RE\mathrm{Al}_{1-x}\mathrm{Ge}_3$ (RE = Nd, Sm, Gd, Tb, Dy, Ho; $0.6 < x < 0.9$). A tale of vacancies at the Al sites and the concomitant structural modulations

Jiliang Zhang,[a] Yanyan Liu,[b] Chan Hung Shek,[c] Yingmin Wang,[b,] Svilen Bobev[a,*]*

[a] Department of Chemistry and Biochemistry, University of Delaware, Newark, Delaware 19716, United States.

[b] Key Laboratory of Materials Modification by Laser, Ion, and Electron Beams (Dalian University of Technology), Ministry of Education, Dalian University of Technology, Dalian 116024, Liaoning, P. R. China.

[c] Department of Applied Physics and Materials Science, City University of Hong Kong, Kowloon, Hong Kong.

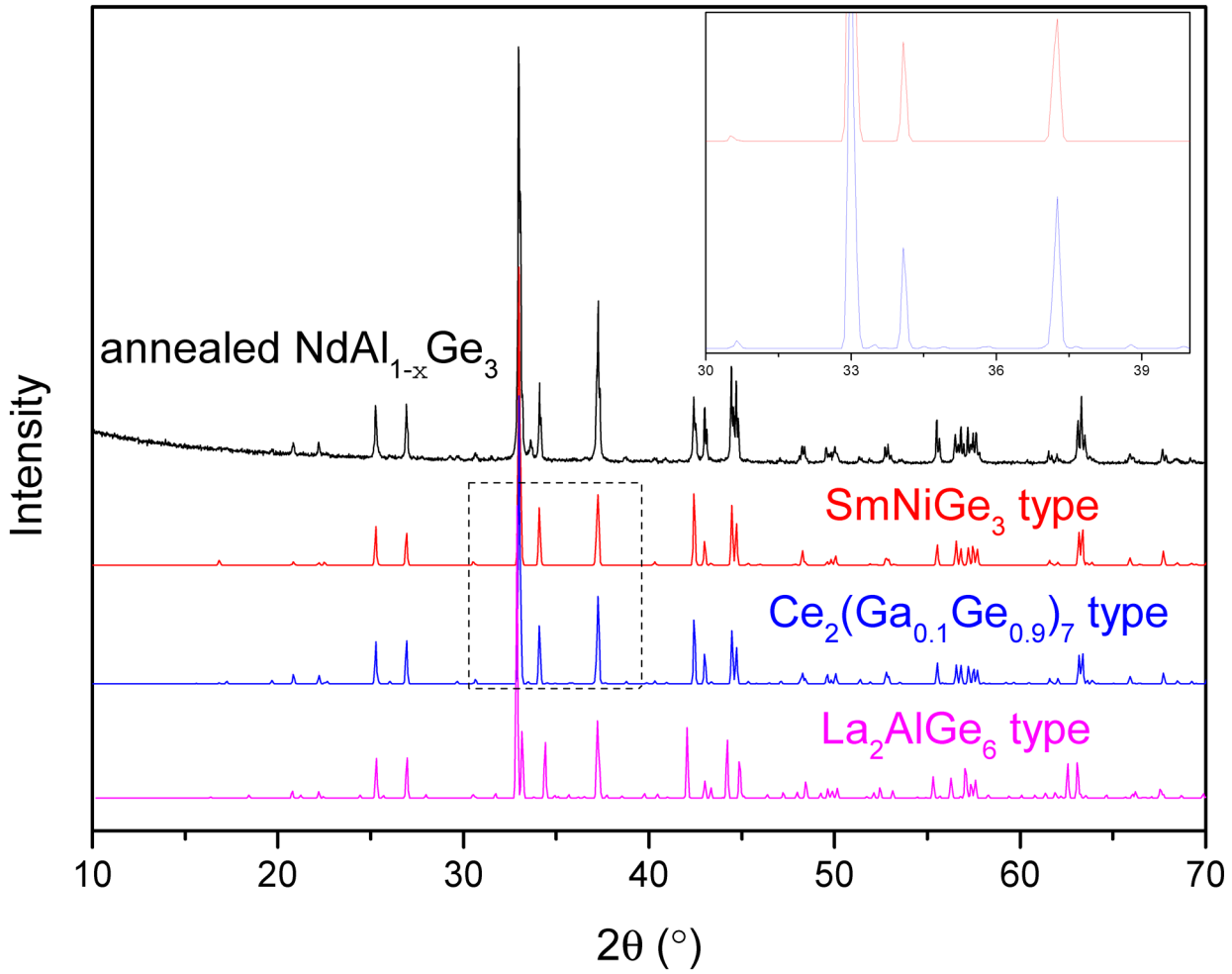

Figure S1. Experimental and simulated X-ray powder diffraction patterns based on three different structures for the $NdAl_{1-x}Ge_3$ compound. The enlarge view in the inset to emphasize the satellites in the $Ce_2(Ga_{0.1}Ge_{0.9})_7$ structure type.

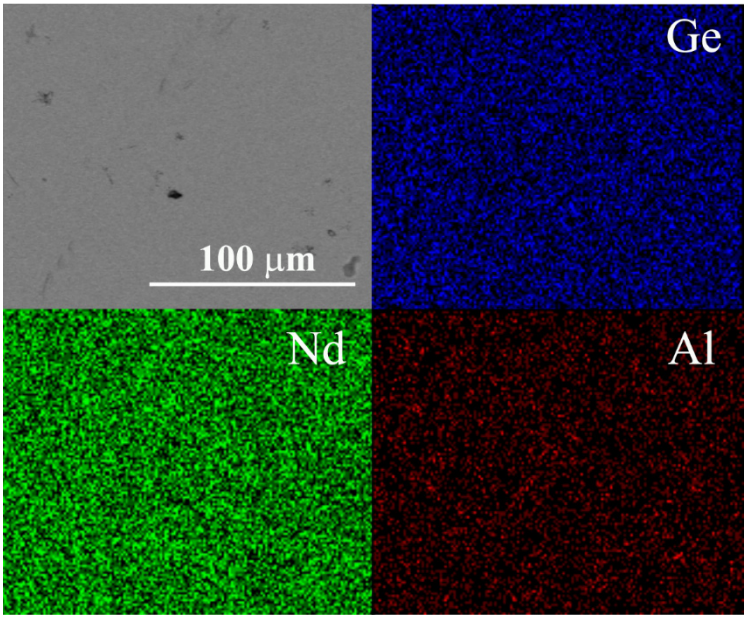

Figure S2. SEM image of a crystal of $NdAl_{1-x}Ge_3$ samples and elemental mapping.

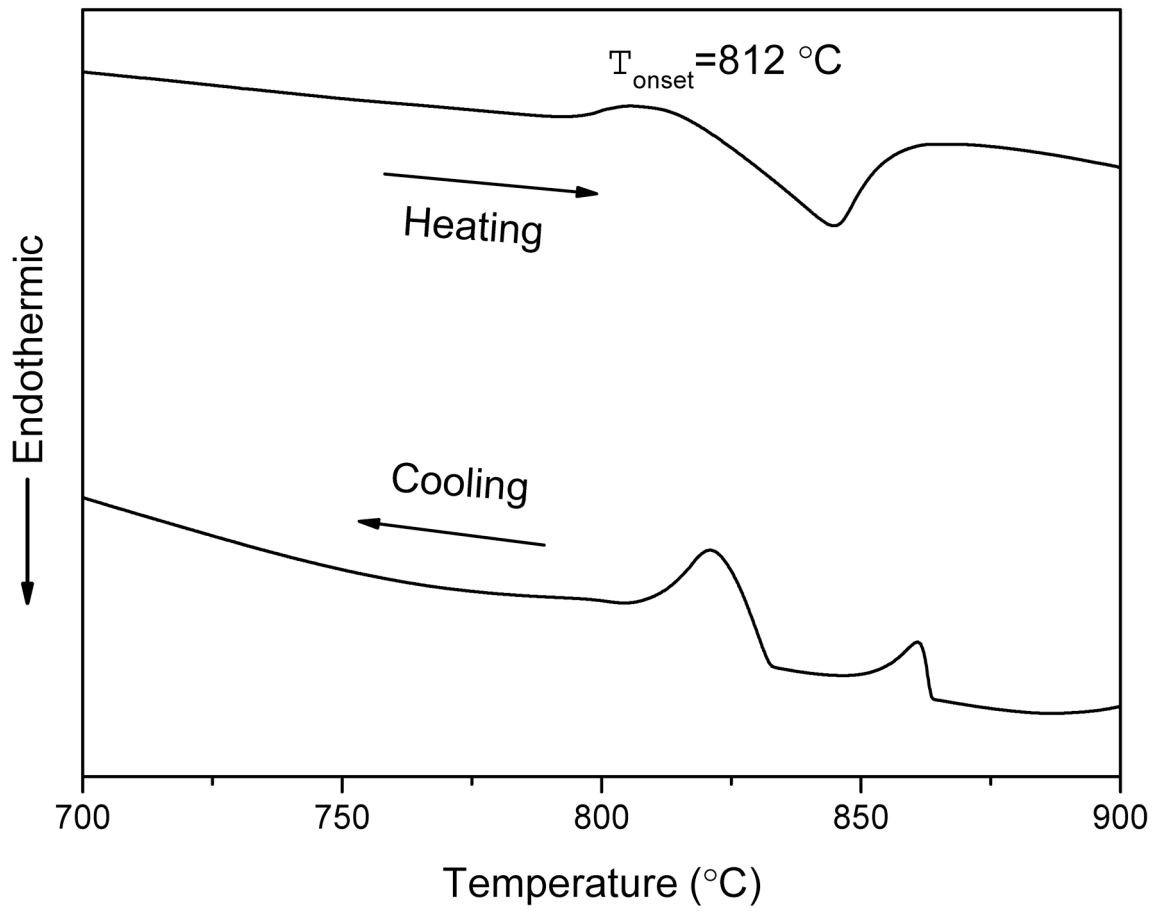

Figure S3. Thermal trace on the melting process of $GdAl_{1-x}Ge_3$ at a heating and cooling rate of 15 K/min.

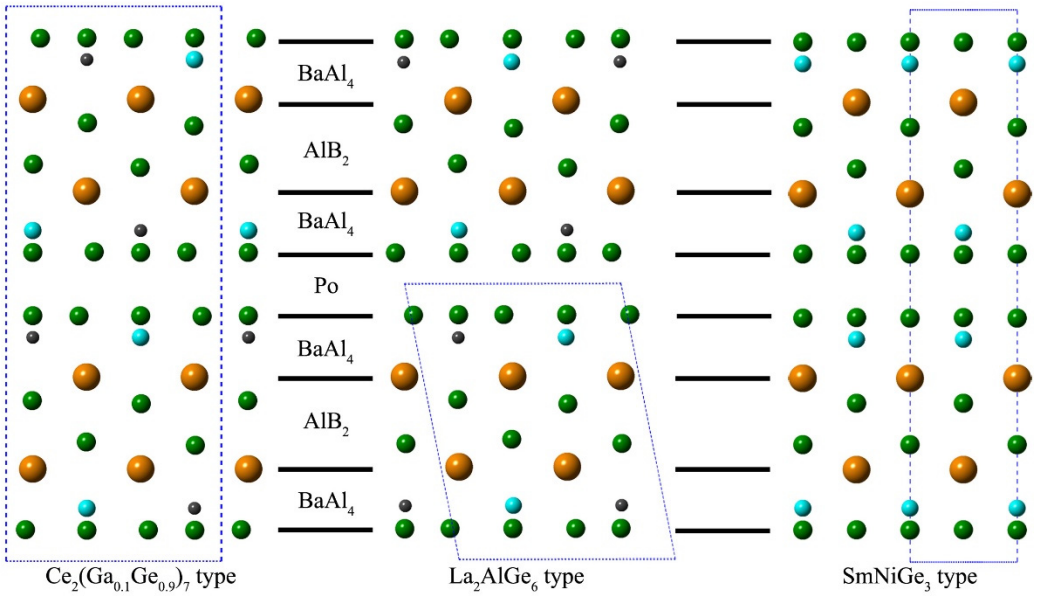

Figure S4. Projections of three types of closely related structures, based on similar building units. To the right, $SmNiGe_3$ structure, viewed along [001]; middle, La_2AlGe_6 structure, viewed along [010]; left, $Ce_2(Ga_{0.1}Ge_{0.9})_7$ structure, viewed along [100]. Black balls show the vacancies, and the colored spheres represent the atoms in structure as follows: orange for the rare-earth metal, green for Ge, and blue for Al. The unit cells are outlined

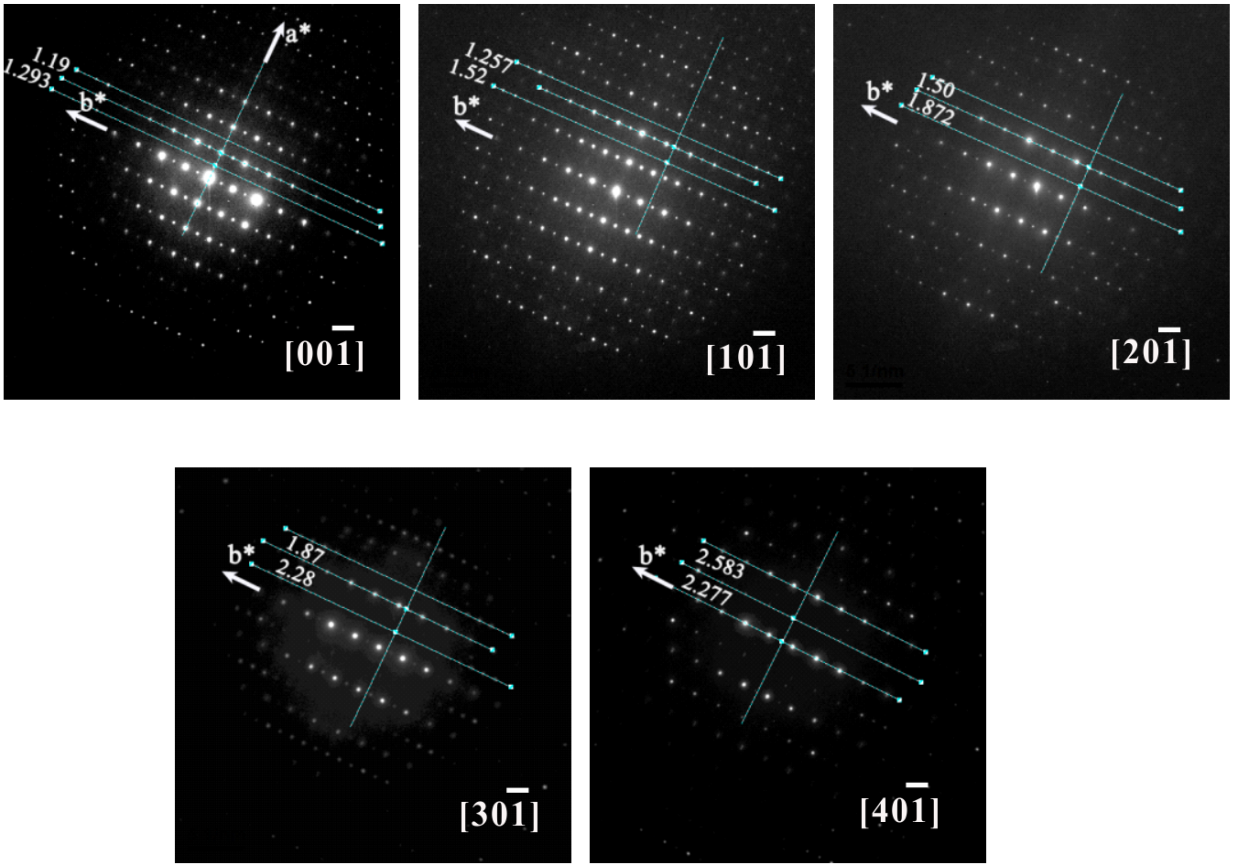

Figure S5. The distances of satellites to adjacent parent reflection rows, measured to show the incommensurate nature of the modulations. These zones correspond to Figure 6 in the main text.

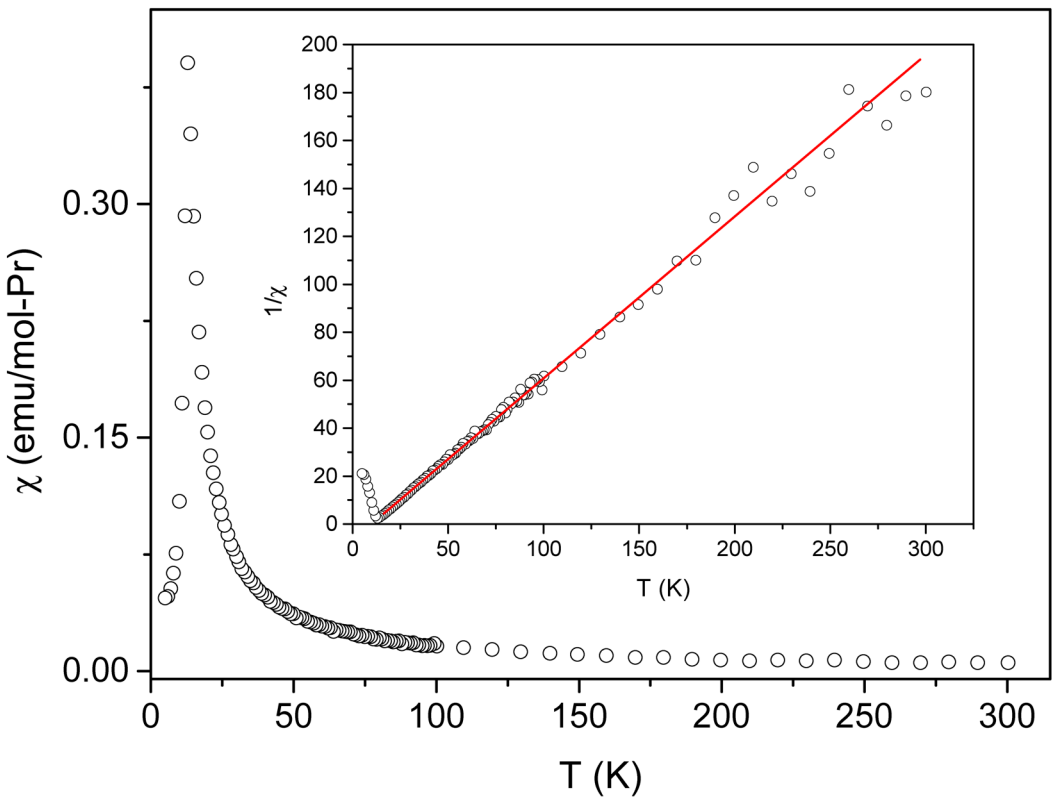

Figure S6. Temperature dependence of the magnetic susceptibility χ(T) for polycrystalline Pr_2AlGe_6 (La_2AlGe_6 type). The inset shows the inverse susceptibility and the red line represents the linear fit to the Curie-Weiss law.

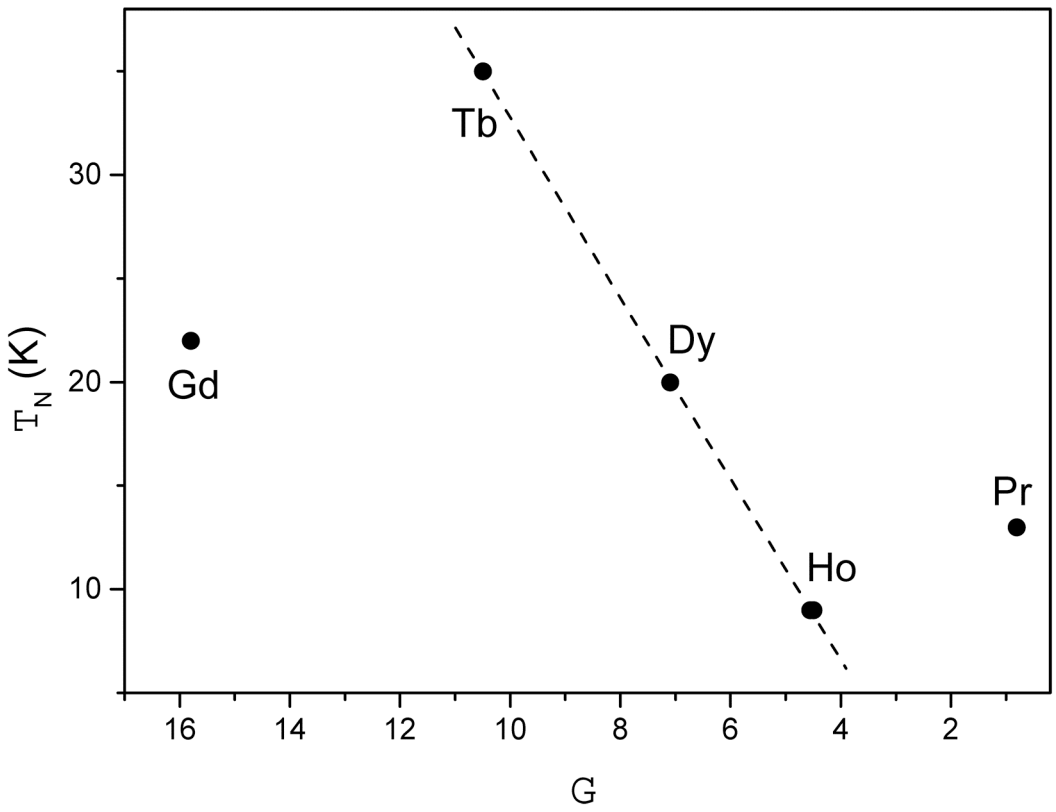

Figure S7. Néel temperatures of $RE\mathrm{Al}_{1-x}\mathrm{Ge}_3$, plotted as a function of de Gennes factors.

Table S1. Selected interatomic distances (Å) in $NdAl_{1-x}Ge_3$,[a] refined using the $SmNiGe_3$-type structure as a model.

Atomic pair	Distance (Å)	Atomic pair	Distance (Å)
Nd–Ge1 (×4)	3.097(1)	Ge2–Al (×2)	2.288(9)
Nd–Ge2 (×2)	3.082(3)	Ge2–Ge2	2.406(4)
Nd–Ge3 (×2)	3.132(3)	Ge2–Ge3 (×4)	2.948(1)
Nd–Al (×4)	3.30(1)	Ge3–Al (×2)	2.194(9)
Ge1–Al	2.43(2)	Ge3–Ge3	2.441(5)
Ge1–Ge1 (×2)	2.574(2)		

[a] Refined occupancy for the Al site is 0.38(4).

[b] It appears that the long Ge2–Ge3 interactions can be subtly affected by the next-nearest neighbors. For example, the distance is reduced from 2.948(1) Å to 2.842(1) Å on moving from the Nd- to the Ho-analog, which must be the combined effect of the unit cell contraction due to an increase number of Al vacancies and the smaller size of the rare-earth element.

Table S2. Principal mean square atomic displacements ($Å^2$) in $NdAl_{1-x}Ge_3$, refined using the $SmNiGe_3$-type structure as a model.

	U_{11}	U_{22}	U_{33}
Nd	0.0051(7)	0.0048(7)	0.0054(7)
Ge1	0.008(1)	0.012(1)	0.006(1)
Ge2	0.010(2)	0.006(1)	0.012(4)
Ge3	0.140(5)	0.008(2)	0.010(2)
Al[a]	0.072(12)	0.010(12)	0.04(1)

[a] Refined occupancy is 0.38(4).

Table S3. Selected interatomic distances (Å) in $NdAl_{1-x}Ge_3$,[a] refined using the $Ce_2(Ga_{0.1}Ge_{0.9})_7$-type structure as a model, following re-integration of the raw single-crystal data and adopting a larger orthorhombic unit cell.

Atomic pair	Distance (Å)	Atomic pair	Distance (Å)
Nd–Ge1	3.150(1)	Ge1–Al	2.448(6)
Nd–Ge2	3.067(2)	Ge1–Ge3	2.490(2)
Nd–Ge2	3.083(2)	Ge1–Ge4 (×2)	2.563(2)
Nd–Ge3	3.142(1)	Ge2–Ge2	2.604(3)
Nd–Ge4	3.091(2)	Ge2–Ge5	2.571(3)
Nd–Ge4	3.093(2)	Ge3–Al	2.459(6)
Nd–Ge5	3.104(2)	Ge3–Ge4 (×2)	2.562(2)
Nd–Ge5	3.119(2)	Ge4–Al	2.518(2)
Nd–Al	3.295(4)	Ge4–Ge4	2.450(1)
Nd–Al	3.308(4)	Ge5–Al	2.509(4)
		Ge5–Ge5	2.534(3)

[a] Refined occupancy is of the Al site is 0.63(2).

Table S4. Principal mean square atomic displacements (Å^2) in $NdAl_{1-x}Ge_3$, using the $Ce_2(Ga_{0.1}Ge_{0.9})_7$-type structure as a model, following re-integration of the raw single-crystal data and adopting a larger orthorhombic unit cell.

	U_{11}	U_{22}	U_{33}
Nd	0.0080(2)	0.0074(2)	0.0070(2)
Ge1	0.0118(5)	0.047(1)	0.0113(5)
Ge2	0.0094(4)	0.0082(4)	0.0099(4)
Ge3	0.0121(5)	0.045(1)	0.0115(5)
Ge4	0.0410(5)	0.0113(3)	0.0095(3)
Ge5	0.0096(4)	0.0083(4)	0.0120(4)
Al[a]	0.010(2)	0.008(2)	0.006(2)

[a] Refined occupancy is 0.63(2).

Table S5. Atomic coordinates of optimized La_2AlGe_6 with the monoclinic La_2AlGe_6-type structure.

Atom	Site	*x*	*y*	*z*
La	8*j*	0.0959	0.2473	0.3334
Ge4	8*j*	0.2805	0.2157	0.1134
Ge1	4*i*	0.1438	0	0.5625
Ge5	4*i*	0.3673	0	0.4296
Ge2	4*i*	0.0669	0	0.1106
Ge3	4*i*	0.4941	0	0.1106
Al	4*i*	0.8021	0	0.2021

Table S6. Atomic coordinates of optimized La_2AlGe_6 with the orthorhombic $Ce_2(Ga_{0.1}Ge_{0.9})_7$-type structure.

Atom	Site	*x*	*y*	*z*
Nd	16*g*	0.2533	0.3629	0.0807
Ge1	8*f*	0	0.1197	0.4670
Ge2	8*f*	0	0.3372	0.3064
Ge4	8*f*	0	0.1281	0.0316
Ge3	16*g*	0.2871	0.1220	0.1935
Ge5	8*f*	0	0.4109	0.1942
Al	8*f*	0	0.1234	0.1496

Table S7. Selected interatomic distances in optimized La_2AlGe_6 with the monoclinic La_2AlGe_6-type structure.

Atomic pairs	Distance (Å)	Atomic pairs	Distance (Å)
La–Ge1 (×1)	3.3634	Ge1–Al (×1)	2.6904
La–Ge2 (×1)	3.2231	Ge1–Ge1 (×1)	2.5875
La–Ge2 (×1)	3.393	Ge1–Ge4 (×2)	2.6473
La–Ge3 (×1)	3.4011	Ge2–Ge2 (×1)	2.5921
La–Ge4 (×1)	3.2734	Ge2–Al (×1)	2.6739
La–Ge4 (×1)	3.3342	Ge3–Al (×1)	2.6358
La–Ge5 (×1)	3.2307	Ge3–Ge3 (×1)	2.5871
La–Ge5 (×1)	3.3179	Ge3–Ge4 (×2)	2.6556
La–Al (×1)	3.4023	Ge4–Al (×1)	2.7221
La–Ge2 (×1)	3.4085	Ge4–Ge4 (×1)	2.6445
La–Al (×1)	3.4552	Ge5–Ge5 (×1)	2.5153

Table S8. Selected interatomic distances in optimized La_2AlGe_6 with the orthorhombic $Ce_2(Ga_{0.1}Ge_{0.9})_7$-type structure.

Atomic pairs	Distance (Å)	Atomic pairs	Distance (Å)
La–Ge1 (×1)	3.3723	Ge1–Al (×1)	2.6464
La–Ge2 (×1)	3.2052	Ge1–Ge3 (×1)	2.6248
La–Ge2 (×1)	3.3217	Ge1–Ge4 (×2)	2.6352
La–Ge3 (×1)	3.4391	Ge2–Ge2 (×1)	2.5398
La–Ge4 (×1)	3.3009	Ge2–Ge5 (×1)	2.6102
La–Ge4 (×1)	3.4062	Ge3–Al (×1)	2.6616
La–Ge5 (×1)	3.2114	Ge3–Ge4 (×2)	2.6116
La–Ge5 (×1)	3.3409	Ge4–Al (×1)	2.7288
La–Ge5 (×1)	3.3568	Ge4–Ge4 (×1)	2.6479
La–Al (×1)	3.4168	Ge5–Al (×1)	2.6782
La–Ge2 (×1)	3.4222	Ge5–Ge5 (×1)	2.6206
La–Al (×1)	3.4901		